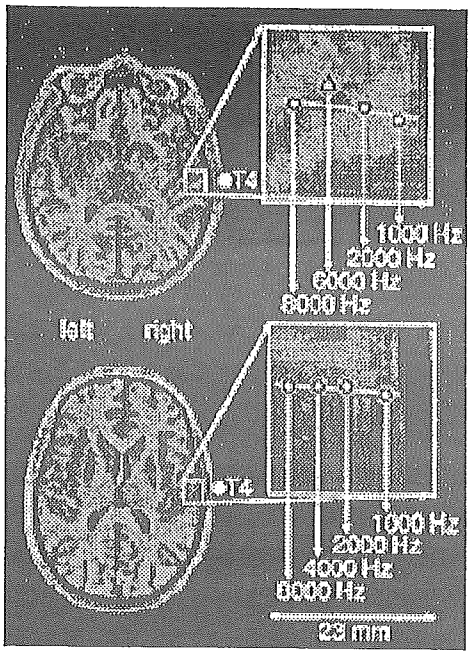

図6　一次聴覚野の各周波数に対応した応答部位
耳鳴りの周波数による音刺激に対する一次聴覚野の応答部位が、耳鳴り患者（上段）において、その空間配列が逸脱していることが、健常者（下段）と比較してわかる　(Muhlnickel et al. 1998 [5] より引用)

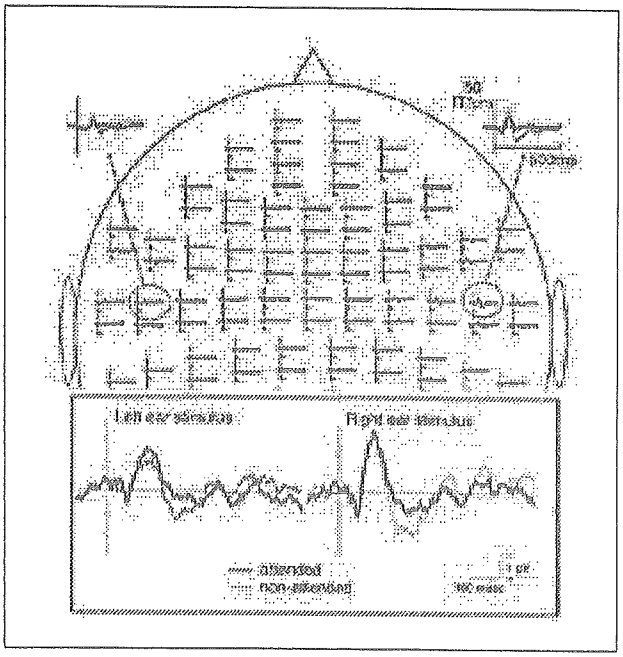

図7　聴覚誘発脳磁場と選択的注意の影響
上段：左耳に呈示された頻回トーンバーストに対する注意関連磁場応答波形。注意関連磁場応答は、両側半球側頭部に認める。赤線および青線：注意および非注意時の応答磁場波形
下段：左右耳それぞれに呈示された頻回トーンバーストに対する頭皮上電極Fzにおける事象関連電位。太線および細線：注意および非注意状態での反応　(Fujiwara et al. 1998 [6] より改変)

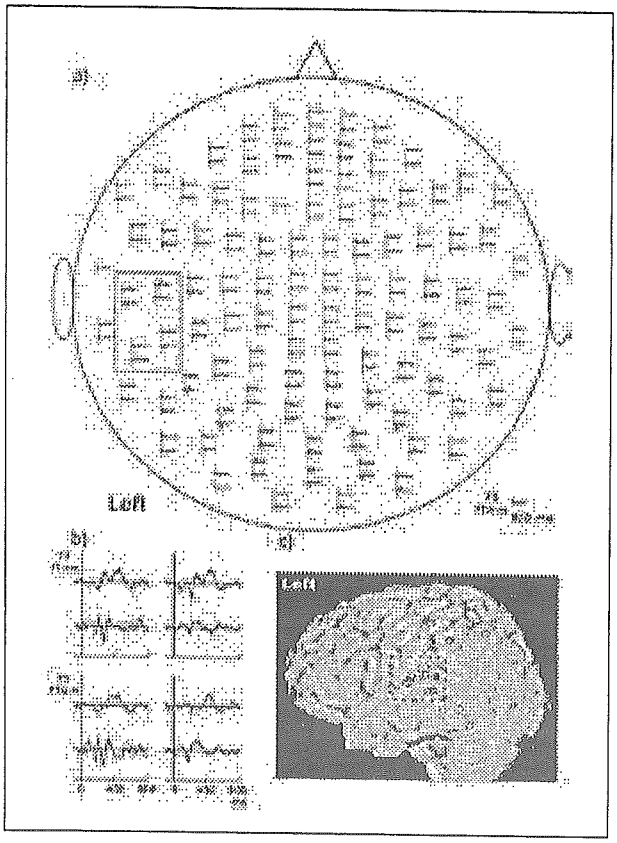

図8　類似語に関連する脳活動
この結果は、類似語の語彙表象へのアクセスが、特に候補語数の多い単語においてより多く、その処理が左上側頭部において行われていることを示唆するものであると考えられる
(Sekiguchi et al. 2003 [10] より改変)

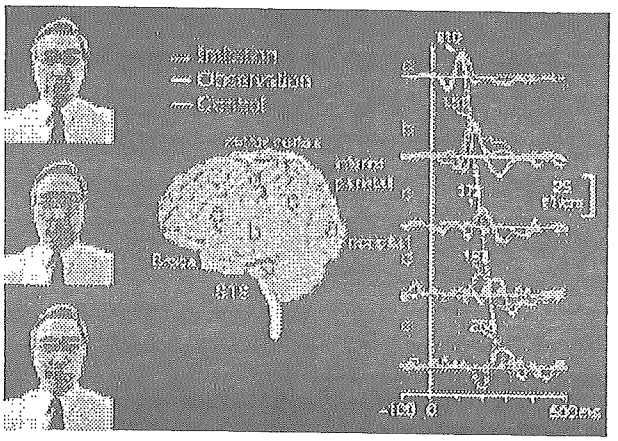

図9　口唇形状の観察・模倣における脳磁場応答波形と主要活動部位（左半球）
大脳皮質内では、後頭部、上側頭溝、下頭頂部、後下前頭部（ブローカ野）、一次運動野の順に活動することが明らかになった。言語性口唇形状の同様の課題、また右半球においても同様の活動を認めた。模倣において、後下前頭部（ブローカ野）、一次運動野で活動が有意に大きくなることを認めている　(Nishitani and Hari, 2002 [14] より改変)

動は、最初に後頭部が、次にブローカ野（特にブロードマン44野）、左側運動野、そして右側運動野の順に活動を認めた。また口唇形状のみを変化させた顔の静止画像の観察、模倣課題時での活動は、後頭部視覚野、上側頭溝、下頭頂部、ブローカ野、そして一次運動野の順に認められた。いずれの場合も、ブローカ野と一次運動野の活動の大きさは、模倣課題時で最大であった。左半球の活動は、言語化可能な口唇形状に対する課題のほうが言語化不可能な口唇形状に対するより優位であり、右半球ではその逆であった（図9、p15）。

さらに、模倣困難を呈するAsperger syndromeの患者における口唇形状の模倣時の脳活動を、健常者の結果と比較した[15]。それによると、両側半球のブローカ野と運動野の活動は有意に小さく、かつ応答潜時が遅延していた。この結果は、Asperger syndromeの模倣障害、新しいスキルの獲得における障害の機序を考えるうえで貴重なデータと考えられる。

他人の動作、もしくは動作を示唆する静止画像・写真を観察している場合でも、自ら同様の動作を遂行したときのように、これらの領域が活動することを示しており、他人の動作をあたかも自らの動作として映し出しているかのようなことから、Human Mirror Neuron System（HMNS）とよんだ[13, 16, 17]。以上の研究は、後下前頭部（BA 44）は動作の理解とその再現に重要な役割を担っていることを示唆するものである。

MEGは完全な非侵襲的記録法で反復記録が可能であること、優れた時間・空間分解能を保有していること、MEG計測装置の多チャンネル化が実現したことなどから、臨床検査法のひとつとして確立されつつある。今後、fMRIなどの他の脳機能評価方法との有機的連携により、脳機能に関連する研究と臨床応用に貢献するものと期待されている。

文　献

1) De Renzi E, Prosopagnosia. In: Feingerg TE, Farah MJ, editors. Behavioral Neurology and Neuropsychology. NewYork: MacGraw-Hill; 1997. p. 245-55.
2) Halgren E, Raij T, Marinkovic K, Jousmaki V, Hari R. Cognitive response profile of the human fusiform face area as determined by MEG. Cereb Cortex 2000; 10 (1): 69-81.
3) Perenin M-T. Optic ataxia and unilateral neglect. In: Their P, Karnath H-O, editors. Clinical evidence for dissociable spatial functions in posterior parietal cortex. Parietal lobe contributions to orientation in 3D space. Berlin: Springer-Verlag; 1997. p.289-308.
4) Nishitani N, Uutela K, Shibasaki H, Hari R. Cortical visuomotor integration during eye pursuit and eye-finger pursuit. J Neurosci 1999; 19 (7): 2647-57.
5) Muhlnickel W, Elbert T, Taub E, Flor H. Reorganization of auditory cortex in tinnitus. Proc Natl Acad Sci USA 1998; 95 (17): 10340-3.
6) Fujiwara N, Nagamine T, Imai M, Tanaka T, Shibasaki H. Role of the primary auditory cortex in auditory selective attention studied by whole-head neuromagnetometer. Brain Res Cogn Brain Res 1998; 7 (2): 99-109.
7) Dhond RP, Buckner RL, Dale AM, Marinkovic K, Halgren E. Spatiotemporal maps of brain activity underlying word generation and their modification during repetition priming. J Neurosci 2001; 21 (10): 3564-71.
8) Simos PG, Breier JI, Zouridakis G, Papanicolaou AC. Assessment of functional cerebral laterality for language using magnetoencephalography. J Clin Neurophysiol 1998; 15 (4): 364-72.
9) Papanicolaou AC, Simos PG, Breier JI, Zouridakis G, Willmore LJ, Wheless JW, et al. Magnetoencephalographic mapping of the language-specific cortex. J Neurosurg 1999; 90 (1): 85-93.
10) Sekiguchi T, Nishitani N, Nakajima Y. Effect of neighborhood size on cortical magnetic responses during word completion task. Neurosci Res 2003; 46 (Suppl 1): S168.
11) Helenius P, Salmelin R, Service E, Connolly JF. Semantic cortical activation in dyslexic readers. J Cogn Neurosci 1999; 11 (5): 535-50.
12) Salmelin R, Schenitzler A, Schmitz F, Freund HJ. Single word reading in developmental stutterers and fluent speakers. Brain 2000; 123 (6): 1184-202.
13) Nishitani N, Hari R. Temporal dynamics of cortical representation for action. Proc Natl Acad Sci USA 2000; 97 (2): 913-8.
14) Nishitani N, Hari R. Viewing lip forms: Cortical dynamics. Neuron 2002; 36 (6): 1211-20.
15) Nishitani N, Avikainen S, Hari R. Abnormal imitation-related cortical activation sequences in Asperger's syndrome. Ann Neurol 2004; 55 (4): 558-62.
16) Hari R, Nishitani N. From viewing of movements to understanding and imitation pf other person's acts: MEG studies of the human mirror-neuron system. In: Kanwisher N, Duncan J, editors. Functional neuroimaging of visual cognition: Attention and Performance XX. New York: Oxford Univ. Press; 2004. p.463-79.
17) Nishitani N, Schürman M, Amunts K, Hari R. Broca's region: From action to language. Physiology 2005; 20 (2): 54-63.

MEG

MEG(Magnetoencephalography)

室長
西谷　信之
Nobuyuki NISHITANI

国立身体障害者リハビリテーションセンター研究所感覚機能系障害研究部感覚認知障害研究室

KEY WORDS

脳磁場計測
MEG
脳磁図
脳機能評価
臨床応用

SUMMARY

優れた時間並びに空間分解能を有し，頭部の構造物による信号の歪みがない脳磁場計測法は，基礎的な脳機能解明に加えて，腫瘍性疾患やてんかんなどの術前評価のみならず，他の脳疾患においても非侵襲的臨床検査法としてしだいに応用されつつある．

はじめに

脳磁場計測(magnetoencephalography：MEG)による頭蓋外からの微弱脳磁場の計測が行われたのは，脳波の出現後40年を経た1960年代後半のことであった．その後1970年代に超伝導量子干渉素子装置が開発され，脳磁場計測がより現実的なものとなった．その結果，電気的な基準を必要とせずにヒト脳の随意脳活動や誘発磁場信号の記録が可能となった．更に近年の科学技術の急速な進歩により，記録センサーの増加と解析法が進化し，脳機能解明研究とともに臨床応用が進められている．

脳磁場の発生機序

脳機能の解明においては，脳活動の時間的関係を明らかにすることが重要である．MEGは，ミリ秒(msec)レベルの時間分解能を保有し，脳機能のダイナミクスを解明することが可能な非侵襲的手法である．

ヒトの脳より発生する磁場は地球の定常磁場の約1億分の1に相当する非常に弱い信号であるため，頭皮上で計測されるためには，神経配列に規則性を持った神経細胞の一群が同期して発火する必要がある．大脳皮質運動野第Ⅴ層に存在する錐体細胞は，細胞体から皮質表層に向かって樹状突起が分布している．MEGが計測する脳磁場は，主としてこの大脳皮質錐体細胞への興奮性シナプス後電位(excitatory postsynaptic potential：EPSP)により生じる細胞内電流によるものである．

現在ほとんどのMEGでは，頭皮と平行に計測コイルが設置され，そのコイルを貫く磁場をもとに，頭皮上の磁場分布並びに脳活動を評価している．脳溝に位置し，脳表に平行な尖樹状突起内の細胞内電流が形成する垂直方向の磁場成分をMEGは記録するのに対して，EEGは脳表に対して垂直水平両

方向の細胞外容積電流を計測することから，両者は相補的な関係にある．

EEGに勝るMEGの最大の利点は，電位分布には影響を与える，頭蓋の構造物による磁場信号の歪みを認めない点である．頭蓋骨，脳脊髄液，脳，硬膜などの頭部の構成組織の透磁率は均一と見なされるため，頭部術後や頭部挫傷後などの構成組織の変化による頭皮上の磁場信号とその分布には歪みが生じない．その結果，MEGは密度の高い細胞内電流を計測することとあわせて，脳内活動源を数mm以内の誤差で推定することができる．また，EEGは基準電極に対する相対的な量を測定するのに対して，MEGは絶対量である磁束密度を計測しているため，基準を必要としない．一方MEGの欠点は，表面的な活動源を良好に限局できるが，磁場強度が距離の2乗ないし3乗に反比例して急速に減衰するために，深部活動減の限局を苦手とする．

MEGによる脳機能評価

MEGにより様々な脳機能の解明研究が精力的に進められ，多くの知見が得られている(表1)．

表1　脳磁場計測による脳機能評価

自発脳磁場活動
　睡眠時脳磁場活動
　発作性脳磁場活動
誘発脳磁場活動
　一次体性感覚，聴覚，視覚誘発磁場活動
高次脳磁場活動
　注意，記憶，認知，言語，計算，学習
運動関連脳磁場活動
感覚運動連関脳磁場活動

1．背景自発脳活動

背景自発脳活動に認められる周波数がそれぞれ種々の脳活動を反映していることは知られているが，MEGによる脳機能評価としての特徴は，機能局在と同時に脳活動のリズムを明らかにできることである．例えば，運動皮質に認められる20Hzや40Hz帯域のリズムと筋放電との相関は，随意運動の運動野支配の機序や運動神経疾患の病態生理を理解する上で重要である．睡眠時第2段階に認められる紡錘波の頭皮上分布と周波数に基づく発生機序の解明にも，MEGは応用されている．

2．体性感覚誘発磁場(somatosensory evoked magnetic field：SEF)

末梢神経電気・触覚刺激により，刺激後20～30msecで早期SEF(N20m)が，35～70msecで後期SEF(N40m，P60m)が誘発され，刺激対側半球の中心後回に存在する一次体性感覚野（SⅠ)の3b野と1野に，それぞれ主活動源が推定されている[1]．シルビウス裂とローランド溝交差部後方の二次体性感覚野(SⅡ)は，両側からの感覚入力を受ける[2]．痛覚刺激によるSEFは1野由来とされている[3]．痛覚刺激では，刺激対側のSⅠとSⅡおける反応開始が刺激後約130msec前後でほとんど同時であることから，視床から平行してSⅠとSⅡに投射すると考えられる．

3．視覚誘発磁場(visual evoked magnetic field：VEF)

パターン反転全視野刺激により，N75m，P100m，N145mの発生源が後頭葉烏距溝外側部付近に，また片眼のフラッシュ刺激では健常者で両側後頭葉に活動源が推定されている[4]．上4分の1視野刺激より下4分の1視野刺激の方が，50～70msec後に出現する後頭葉烏距溝の活動は大きく，半視野刺激によるVEFは下4分の1視野刺激によるそれに類似していることから，複雑な視覚情報処理過程は下視野が優勢である[5]．動きに対しては両側後外側側頭部(MT/V5)に活動源が推定されている[6]．

4．聴覚誘発磁場(auditory evoked magnetic field：AEF)

刺激後約50msecで中潜時AEF(P50m)が対側優位に出現し，100msecで誘発されるAEF(N100m/N1m)は，刺激同側におけるAEFよりも対側のそれの方が短潜時(約10msec)，高磁場で，その電流源はともに両側上側頭回(Heschl回)に推定されている．また，純音刺激に対するAEFは左半球に比べて右半球の方が短潜時，高磁場である．空間的に配置された音源からの音刺激に対するAEFは右半球一次聴覚野の優位性が示されている[7]．刺激音の周波数とN100mの推定発生源の位置との関係では，周波数が高くなるに従って推定電流源は深くなる(spatial tonotopy)．

5．注意(attention)

我々は騒音のなかにいても，ある特定の音や声を聞き分けることが可能である(カクテルパーティー現象)．左右いずれの耳へ選択的に注意を向けても，一次聴覚応答N100mの応答潜時には変化が認められないが，それぞれの振幅及び推定される活動源の大きさが有意に増大する[8]．この結果は特定の音に対して選択的に注意を向けることで，一次聴覚野の活動が亢進したために生じた現象であることを示している．

6．言語(language)

視聴覚提示された語の了解や語の作成にかかわる脳活動の時間的流れも(一次視聴覚野から側頭部，下頭頂部，

後下前頭部そして運動野)，全頭型MEGの出現により明らかになった[9][10]．失読症患者では，後頭内側部の活動(単語呈示後約100msec)は健常者と変化が見られなかったが，文脈での単語の意味づけの段階(約150～200msec)で障害されていた[11]．文脈全体で単語を認識処理する過程が健常者と失読症患者では異なることを示唆している．更に，中・後側頭部，下頭頂部そして後下前頭部における呼称，音韻処理，単語想起などに関連する詳細な言語機能の知見が得られている[12][13]．単語の音読では，類似語数の多い単語が刺激提示された場合で，より強度に脳活動が賦活された[14]．母音刺激では左半球での応答が有意であることから，特に単語認識課題でのMEGの応答並びにその活動源推定結果とWadaテスト[15]との比較を行い，MEGは言語優位半球の非侵襲的同定に有用であるとの報告もなされている[16][17]．左半球における言語特異領域が，動静脈奇形や部分切除術後に右半球の相当部位や左半球の後部に移動していたとする報告もあり，言語領域の可塑性を示唆している[18]．

7．認知(cognition)

一般に深部領域からの磁場信号の記録は困難とされている．内側側頭部に位置する海馬や扁桃体もその1つである．しかし，てんかん源性発作波に比べて後期誘発成分は頭皮上に波及しやすく，誘発波形の加算によりS/N比を向上させることで磁場信号の記録は可能となる．聴覚オッドボール課題で，認知機能を反映すると考えられているP300に相当する応答磁場波形の発生源が，健常者や難治性てんかん患者の選択的切除術前後の記録から，両側半球の側頭葉内側部(海馬)，上側頭部と下頭頂部に推定されている[19][20]．顔の認知に関しては，機能画像などにおいても研究が進んでおり，特に右紡錘状回が特異的に活動すると報告されている．MEGでの研究では，顔刺激後約120msecで右紡錘状回を含む後下側頭部が活動するとされている[21]．

8．運動関連脳磁場(movement-related cortical magnetic field：MRCF)

随意運動に伴って頭皮上から記録される運動関連脳電位に相当する脳磁場活動として，運動関連脳磁場(movement-related cortical field：MRCF)が知られている[22]．手指などの随意運動時には，運動開始約1～1.5秒前より運動対側優位に，EEGでのbereitschaftspotential (BP)に相当する磁場(readiness field：RF)が記録され，RF終点近傍の磁場はmotor field (MF)とされている．RFの運動開始前200～900msecで中前頭葉(Brodmann 9野)に，またそれに引き続いて補足運動野，前運動野，一次運動野(the primary motor cortex：M1)の順に電流源が推定されている[23]．運動後の活動として，movement evoked field Ⅰ & Ⅱ (MEF Ⅰ & Ⅱ)があり，MFとMEF Ⅰの電流源はそれぞれ中心溝前壁，後壁に推定され，運動野と感覚野の関連が示唆されている[24]．MFは皮質脊髄路の活動に密接に関連し，post-MFは求心性感覚入力による皮質活動を表していると考えられる．更に運動同側のMFが感覚入力によって干渉されることから，運動野と感覚野の相互作用が両半球において平行して生じていることが示唆される[25]．運動時のM1の活動は，運動対側のみならず同側M1においても認められ，その活動の大きさは対側優位である[26]．M1における手指の領域と利き手の関係では，利き手対側の“優位”M1における手指の占める領域が同側よりも広いことが知られている[27]．

9．感覚運動連関脳磁場活動

普段我々は，視聴覚・触覚などの一次感覚情報を受容野より受け入れ，脳内での情報処理を経て，感覚入力に応じた応答を一次運動野の活動として運動器官を通して表現している．

眼球と手指による標的の滑動性追跡眼球運動時には，両側半球で後頭部，前下頭頂部，外側前頭部，そして上頭頂部の順に活動する．前下頭頂部が最大に活動しており，連続する滑動性追跡運動の制御には，前下頭頂部が重要であることが示唆された[28]．手指の動きや口唇形状のみを変化させた顔の静止画像の観察，模倣，並びに自動動作に同期した脳活動について明らかにされている[29][30]．手指の動作の観察にかかわる脳活動は，最初に後頭部が，次に前頭葉後下部：ブローカ野(特にBrodmann 44野)，左側運動野，そして右側運動野の順に活動を認めた．また口唇形状のみを変化させた顔の静止画像の観察，模倣課題時での活動は，両側半球の後頭部視覚野，上側頭溝，下頭頂部，ブローカ野，そして一次運動野の順に認められた．いずれの場合も，ブローカ野と一次運動野の活動の大きさは模倣時で最大であった．左半球の活動は，言語化可能な口唇形状の写真提示の方が言語化不可能なそれに対するより優位であり，右半球ではその逆であった．他人の動作もしくは動作を示唆する静止画像・写真を観察している場合でも，自ら同様の動作を遂行した時のように，これらの領域が活動することを示しており，他人の動作

をあたかも自らの動作として映し出しているかのようなことから，Human Mirror Neuron System (HMNS) とした[29)31)32)]．以上の結果は，後下前頭部(BA 44)が動作の理解とその再現に重要な役割を担っていることを示唆する[31)32)]．

MEGの臨床応用

MEGによる脳機能解明研究に基づいて臨床応用が進行しつつある．MEGによる脳機能評価の対象となり得る疾患は，表2に示すように多彩である．これまでは，中枢占拠性病変の術前脳機能評価，中心溝同定や，てんかん源性発作波焦点の同定が臨床応用の中心であった．しかし近年，術後や脳梗塞などによる機能障害の病態解明のみならず，術後や発症後の経時的記録により，脳機能の可塑性，代償機能の機序解明や，それに基づく機能訓練を含めた治療方針の確立，決定に客観的なデータを提供するなど，その臨床応用が拡大しつつある．

1．背景自発脳磁場

先に述べたように，背景自発脳活動に認められる周波数は，それぞれ種々の脳活動を反映している．アスペルガー症候群(AS)の患者に動作の模倣課題を課した場合，健常者と同様に20Hz帯域の脳活動を一次運動野に認めた[33)]．これは，ASにおける模倣障害は運動皮質の障害ではないことを示唆している．また，耳鳴，パーキンソン病，うつ病などの疾患では，θ波帯域のリズムが増加しているが，これは感覚運動や認知機能に関与しているとされるγ帯域のリズムとの，視床皮質における不均衡によるものであると考えられている[34)]．また，アルツハイマー病(AD)では後頭部優位のαリズムが減衰し，前頭中央部で徐波成分の増大を認める．このように，基礎律動の変化から，疾患特異的な領域を有さない中枢神経疾患の病態が明らかになりつつある．単純ヘルペス脳炎の病初期に認められる自発背景活動の減衰と病巣部に一致した周期的鋭波や，視床内側部の梗塞例でローランド領域のリズム異常を認める[35)36)]．またEEGと同じ周波数帯域で，中心頭頂紡錘波を両側半球で評価することができ，両側半球の中心溝の前後に活動源が推定されている．一側視床に脳梗塞などの病変が存在する場合，一側半球上に認められる紡錘波の分布や振幅が影響を受ける．これらの所見は皮質上に認められる律動と視床との関係を示唆するものである．

表2　脳磁場計測による脳機能評価の対象となり得る疾患

- 頭蓋内占拠性疾患
  - 脳腫瘍
- 発作性疾患
  - てんかん
  - 片頭痛
  - 一過性全健忘
  - めまい
  - 耳鳴
- 痴呆(認知症)性疾患
  - 脳血管性痴呆(認知症)
  - アルツハイマー病
  - 軽度認知障害
  - その他の認知症
- 脳血管障害
  - 脳梗塞
  - 脳出血
  - 一過性脳虚血発作
  - 先天性血管奇形－脳動静脈奇形，もやもや病
- その他
  - うつ病，PTSDなどの精神疾患
  - 頭部外傷後障害
  - 高血圧，糖尿病，高脂血症，心疾患，血液疾患などのハイリスクグループ

2．てんかん(発作性脳磁場)

てんかん発作間歇期の異常波からの信号源推定はMEGの臨床応用の初期から行われ，難治性側頭葉てんかんの焦点同定やてんかん外科における術前診断にMEGは威力を発揮している．Landau-Kleffner症候群のように両側性に発作波を認める場合でも，全頭型MEGの出現により，てんかん源性発作波の焦点が両側シルビアン裂内側の皮質に推定できるようになった[37)]．局所性大脳皮質形成異常の症例でも，巨大細胞と大好酸性細胞を認める皮質に，深部電極記録で同定したてんかん源性焦点に一致してMEGでも焦点が推定され，MEGの有用性が示されている[38)]．側頭葉内側部などの脳深部からの異常波の局在診断はMEGの性質上困難を伴うが，てんかん源性神経活動を双極子の方向によって，てんかん易誘発部位を明らかにすることができ，部分切除術前診断に有効である[39)]．また，脳領域の部分切除術後においても，頭骸骨や硬膜の欠損による信号の歪みがないため，てんかん源性活動の再評価に有用である[39)]．

3．誘発脳磁場

SEFによる脳機能メカニズムの解明のみならず，機能代償，機能予後の評価が行われている．一側頭頂部梗塞例において，正中神経電気刺激により同側半球のSⅠ並びにSⅡの応答が異常で，健側SⅡのSEFが正常に誘発されたことから，刺激対側ではSⅠとSⅡが連続的に活動するのに対して，刺激同側のSⅡでは，刺激末鞘神経から直接感覚入力を受けると考えられた[40)]．一方，SⅠとSⅡの反応がほぼ同じ潜時(刺激後約20～30msec)で誘発され，SⅠからSⅡへの遠心路以外に，SⅡへ

の視床皮質投射路の存在の可能性も示唆されている[41]．

皮質反射性ミオクローヌスに認められる巨大SEPの起源は，3b野に加えて中心溝前壁であり，感覚運動野の病的興奮がその病態であることがMEGで明らかになった[42]．ADとLennox-Gastaut症候群に認められる，中心前野に由来する自発性ミオクローヌスの頭皮上極性を比較し，皮質性ミオクローヌスとは異なる中心前野の層状構造の活動様式が示唆された[43]．これらの結果は病態解明に基づく治療への道を切り開くものである．

感覚野領域に発生した脳梗塞例では，障害側のみならず，健側においても感覚野領域が拡大することがあるが，両半球の感覚野領域が非対称であるほど，臨床的予後が不良という[44]．左前頭・頭頂ローランド領域に動静脈奇形を有する症例で，右半身での感覚刺激に対する応答が，右半球の下頭頂部から島周辺にかけて，左半身からの刺激に対するものと同様に体性局在分布を認めた．また，左側頭・頭頂部に出生前から梗塞を持つ脳性麻痺例で，右手への触覚刺激に対して両側半球のSⅠにSEFが誘発され，左手刺激による右SⅠにおけるSEFの局在配列は空間的に縮小していた[45]．

4．視覚機能障害

フラッシュ刺激はパターン刺激と異なり固視する必要がないため，小児や視野測定が困難な頭蓋内病変を有する症例に対する多角的な視野の検査として有用で，MEGにおいても半盲の他覚的検査として用いられている．

相貌失認の主病巣部位は後側頭下内側部紡錘回，特に右側であると言われている[46]．MEGによる顔認知の評価では，顔写真の刺激後約160msec前後で紡錘回に活動を認めており[47]，相貌失認の非侵襲的診断の可能性を示唆している．半側空間無視は，右半球頭頂葉が主責任病巣と考えられている[48]．この頭頂部は，視覚運動統合機構において視線，四肢追視運動制御の中心部位であることから，その病態の評価が可能である[28]．

5．聴覚機能障害

環境音と言語音の脳内処理機構は左右半球で異なる．言語音に対する20～45Hzの脳活動は，右半球の活動に比べて左半球後中側頭部や内側側頭部が早期に活動するのに対して，非言語環境音では逆に右半球の方が早期に活動する[49]．耳鳴側とは対側の一次聴覚野においては，健常者に認められるspatial tonotopyが，耳鳴に対応した周波数で逸脱しており[50]，聴覚野における可塑的変化と考えられ，耳鳴の臨床診断と治療の指針となり得る．

AD患者の両耳に純音の反復刺激を与えた際，左半球のN100mの潜時が健常者に比べて有意に遅延しており，ADの皮質機能障害の重症度評価に有用である[51]．吃音は聴覚性のフィードバックの障害が原因であると考えられているが，吃音者では自発的に音声を発する時にN100mの大きさが左右聴覚野において著しく不均衡になっている[52]．

6．運動障害

高次運動機能障害として，運動失行や口部顔面失行などの失行は麻痺，不随意運動，失調などの障害に伴う運動器官の異常がないにもかかわらず，目的に沿った運動・動作を遂行できない病態で，言語命令，模倣命令のいずれにおいても運動・動作の再現ができない．つまり失行は，運動・動作の理解の障害が存在するのではないかと考えられる．AS患者では，この部位の活動が健常者に比べて有意に小さく，かつ応答潜時が遅延していた[53]．これらは，失行やASの病態生理解明，診断に繋がるものと期待される．

7．言語機能障害

失読症では，文脈中の語彙理解に関係すると考えられる左上側頭部の活動が，健常者に比べて約100msec遅くかつ小さい[54]．これは言語処理の前段階での障害によると考えられ，健常者と失読症患者では，文脈全体で単語を認識処理する過程が異なることを示唆している．単語の発話は，健常者では刺激提示後400msec以内に左下前頭部，左運動野，運動前野の順に活動するのに対し，吃音者ではこの順序が逆になっている[55]．また，健常者では発話中に右運動野と運動前野の活動も認められるが，吃音者では認められなかった[55]．

左側被殻，島の出血後梗塞により運動性失語を呈した症例で，言語機能回復訓練開始前と1ヵ月後でのブローカ野の活動の変化を比較したところ，機能訓練後のブローカ野の活動は健常者に比べて遅延しているものの(25～50msec)，増強していた．このことは機能訓練に伴う脳機能の客観的な評価にMEGが有効であることを示している．

おわりに

MEGの臨床応用は，ようやく途に着いたばかりであるが，高い時間空間分解能を持つMEGの脳機能評価にお

ける有用性は証明されてきた．臨床応用においては，体内に金属を保有する場合には計測が困難であり，また，てんかんの重積発作時や脳虚血発作急性期などの病態によって検査が不可能となるといった制約や，活動源の電流の方向により評価が困難であるなど，MEGによってすべての脳機能が評価されるわけではない．したがって，従来の脳機能評価法や近年の脳機能イメージングと連携を図り，診断などに供していくことが肝要である．

文　献

1) Hari R, Forss N : Magnetoencephalography in the study of human somatosensory cortical processing. Philos Trans R Soc Lond B Biol Sci **354** : 1145-1154, 1999
2) Simoes C, Hari R : Relationship between responses to contra- and ipsilateral stimuli in the human second somatosensory cortex SII. Neuroimage **10** : 408-416, 1999
3) Ploner M, Schmitz F, Freund HJ, et al : Differential organization of touch and pain in human primary somatosensory cortex. J Neurophysiol **83** : 1770-1776, 2000
4) Shigeto H, Tobimatsu S, Yamamoto T, et al : Visual evoked cortical magnetic responses to checkerboard pattern reversal stimulation : a study on the neural generators of N75, P100 and N145. J Neurol Sci **156** : 186-194, 1998
5) Portin K, Vanni S, Virsu V, et al : Stronger occipital cortical activation to lower than upper visual field stimuli. Neuromagnetic recordings. Exp Brain Res **124** : 287-294, 1999
6) Tikhonov A, Haarmeier T, Their P, et al : Neuromagnetic activity in medial parietooccipital cortex reflects the perception of visual motion during eye movements. Neuroimage **21** : 593-600, 2004
7) Palomaki K, Alku P, Makinen V, et al : Sound localization in the human brain : neuromagnetic observations. Neuroreport **11** : 1535-1538, 2000
8) Fujiwara N, Nagamine T, Imai M, et al : Role of the primary auditory cortex in auditory selective attention studied by whole-head neuromagnetometer. Brain Res Cogn Brain Res **7** : 99-109, 1998
9) Dhond RP, Buckner RL, Dale AM, et al : Spatiotemporal maps of brain activity underlying word generation and their modification during repetition priming. J Neurosci **21** : 3564-3571, 2001
10) Laine M, Salmelin R, Helenius P, et al : Brain activation during reading in deep dyslexia : An MEG study. J Cogn Neurosci **12** : 622-634, 2000
11) Helenius P, Tarkiainen A, Cornelissen P, et al : Dissociation of normal feature analysis and deficient processing of letter-strings in dyslexic adults. Cereb Cortex **9** : 476-483, 1999
12) Pulvemuller F, Assadollahi R, Elbert T : Neuromagnetic evidence for early semantic access in word recognition. Eur J Neurosci **13** : 201-205, 2001
13) Pylkkanen L, Stringfellow A, Marantz A : Newuromagneitc evidence for the timing of lexical activation : an MEG component sensitive to phonotactic probability but not to neighborhood density. Brain Lang **81** : 666-678, 2002
14) Sekiguchi T, Nishitani N, Nakajima Y : Effect of neighborhood size on cortical magnetic responses during word completion task. Neurosci Res **46** (Suppl.1) : S168, 2002
15) Wada J, Rasmussen T : Intracarotid injection of sodium amytal for the lateralization of cerebral speech dominance. Experimental and clinical observations. J Neurosurgery **58** : 266-282, 1960
16) Simos PG, Breier JI, Zouridakis G, et al : Assessment of functional cerebral laterality for language using magnetoencephalography. J Clin Neurophysiol **15** : 364-372, 1998
17) Breier JI, Simos PG, Zouridakis G, et al : Language dominance determined by magnetic source imaging. A comparison with the Wada procedure. Neurology **53** : 938-945, 1999
18) Simos PG, Papanicolaou AC, Breier JI, et al : Insights into brain function and neural plasticity using magnetic source imaging. J Clin Neurophysiol **17** : 143-162, 2000
19) Nishitani N, Nagamine T, Fujiwara N, et al : Cortical-hippocampal auditory processing identified by magnetoencephalography. J Cogn Neurosci **10** : 231-247, 1998
20) Nishitani N, Ikeda A, Nagamine T, et al : The role of the hippocampus in auditory processing studied by event-related electric potentials and magnetic fields in epilepsy patients before and after temporal lobectomy. Brain **122** : 687-707, 1999
21) Halgren E, Raij T, Marinkovic K, et al : Cognitive response profile of the human fusiform face area as determined by MEG. Cereb Cortex **10** : 69-81, 2000
22) Nagamine T, Kajola M, Salmelin R, et al : Movement-related slow cortical magnetic fields and changes of spontaneous MEG- and EEG-brain rhythms. Electroencephalogr Clin Neurophysiol **99** : 274-286, 1996
23) Pedersen JR, Johannsen P, Bak CK, et al : Origin of human motor readiness field linked to left middle frontal gyrus by MEG and PET. Neuroimage **8** : 214-220, 1998
24) Gerloff C, Uenishi N, Nagamine T, et al : Cortical activation during fast repetitive finger movements in humans : steady-state movement-related magnetic fields and their cortical generators. Electroencephalogr Clin Neurophysiol **109** : 444-453, 1998
25) Hari R, Imada T : Ipsilateral movement-evoked fields reconsidered. Neuroimage **10** : 582-588, 1999
26) Babiloni C, Carducci F, Pizzella V, et al : Bilateral neuromagnetic activation of human primary sensorimotor cortex in preparation and execution of unilateral voluntary finger movements. Brain Res **827** : 234-236, 1999
27) Volkmann J, Schnitzler A, Witte OW, et al : Handedness and asymmetry of hand representation in human motor cortex. J Neurophysiol **79** : 2149-2154, 1998
28) Nishitani N, Uutela K, Shibasaki H, et al : Cortical visuomotor integration during eye pursuit and eye-finger pursuit. J Neurosci **19** : 2647-2657, 1999
29) Nishitani N, Hari R : Temporal dynamics of cortical representation for action. Proc Natl Acad Sci USA **97** : 913-918, 2000
30) Nishitani N, Hari R : Viewing lip forms : Cortical dynamics. Neuron **36** : 1211-1220, 2002
31) Hari R, Nishitani N : From viewing of movements to understanding and imitation pf other person' acts : MEG studies of the human mirror-neuron system. *in* Functional neuroimaging of visual cognition. Attention and Performance XX, ed by Kanwisher N, Duncan J. New York, Oxford Univ. Press, 463-479, 2004
32) Nishitani N, Schurman M, Amunts K, et al : Broca's region : From action to lan-

guage. Physiology **20** : 54-63, 2005
33) Avikainen S, Kulomaki T, Hari R : Normal movement reading in Asperger subjects. Neuroreport **10** : 3467-3470, 1999
34) Llinas RR, Ribary U, Jeanmonod D, et al : Thalamocortical dysrhythmia : A neurological and neuropsychiatric syndrome characterized by magnetoencephalography. Proc Natl Acad Sci USA **96** : 15222-15227, 1999
35) Makela JP, Salmelin R, Hokkanen L, et al : Neuromagnetic sequelae of herpes simplex encephalitis. Electroencephalogr Clin Neurophysiol **106** : 251-258, 1998
36) Makela JP, Salmelin R, Kotila M, et al : Modification of neuromagnetic cortical signals by thalamic infarctions. Electroencephalogr Clin Neurophysiol **106** : 433-443, 1998
37) Paetau R, Granstrom ML, Blomstedt G, et al : Magnetoencephalography in presurgical evaluation of children with the Landau-Kleffner syndrome. Epilepsia **40** : 326-335, 1999
38) Morioka T, Nishio S, Ishibashi H, et al : Intrinsic epileptogenicity of focal cortical dysplasia as revealed by magnetoencephalography and electrocorticography. Epilepsy Res **33** : 177-187, 1999
39) Baumgartner C, Pataraia E, Lindinger G, et al : Neuromagnetic recordings in temporal lobe epilepsy. J Clin Neurophysiol **17** : 177-189, 2000
40) Forss N, Jousmaki V : Sensorimotor integration in human primary and secondary somatosensory cortices. Brain Res **781** : 259-267, 1998
41) Karhu J, Tesche CD : Simultaneous early processing of sensory input in human primary (SI) and secondary (SII) somatosensory cortices. J Neurophysiol **81** : 2017-2025, 1999
42) Mima T, Nagamine T, Nishitani N, et al : Cortical myoclonus : sensorimotor hyperexcitability. Neurology **50** : 933-942, 1998
43) Mima T, Nagamine T, Ikeda A, et al : Pathogenesis of cortical myoclonus studied by magnetoencephalopathy. Ann Neurol **43** : 598-607, 1998
44) Rossini PM, Tecchio F, Pizzella V, et al : On the reorganization of sensory hand areas after mono-hemispheric lesion : a functional (MEG) /anatomical (MRI) integrative study. Brain Res **782** : 153-166, 1998
45) Simos PG, Papanicolaou AC, Breier JI, et al : Insights into brain function and neural plasticity using magnetic source imaging. J Clin Neurophysiol **17** : 143-162, 2000
46) De Renzi E : Prosopagnosia. *in* Behavioral Neurologedy and Neuropsychology, ed by Feingerg TE, Farah MJ. New York, MacGraw-Hill, 245-255, 1997
47) Halgren E, Raij T, Marinkovic K, et al : Cognitive response profile of the human fusiform face area as determined by MEG. Cereb Cortex **10** : 69-81, 2000
48) Perenin MT : Optic ataxia and unilateral neglect : Clinical evidence for dissociable spatial functions in posterior parietal cortex. *in* Parietal lobe contributions to orientation in 3D space, ed by Their P, Karnath HO. Berlin, Springer-Verlag, 289-308, 1997
49) Palva S, Palva JM, Shtyrov Y, et al : Distinct gamma-band evoked responses to speech and non-speech sounds in humans. J Neuosci **22** : RC211 : 1-5, 2002
50) Muhlnickel W, Elbert T, Taub E, et al : Reorganization of auditory cortex in tinnitus. Proc Natl Acad Sci USA **95** : 10340-10343, 1998
51) Pekkonen E, Jaaskelainen IP, Hietanen M, et al : Impaired preconscious auditory processing and cognitive functions in Alzheimer's disease. Clin Neurophysiol **110** : 1942-1947, 1999
52) Salmelin R, Schnitzler A, Schmitz F, et al : Functional organization of the auditory cortex is different in stutterers and fluent speakers. Neuroreport **9** : 2225-2229, 1998
53) Nishitani N, Avikainen S, Hari R : Abnormal imitation-related cortical activation sequences in Asperger's syndrome. Ann Neurol **55** : 558-562, 2004
54) Helenius P, Salmelin R, Service E, et al : Semantic cortical activation in dyslexic readers. J Cogn Neurosci **11** : 535-550, 1999
55) Salmelin R, Schenitzler A, Schmitz F, et al : Single word reading in developmental stutterers and fluent speakers. Brain **123** : 1184-1202, 2000

Biological Psychiatry

Neuropsychobiology

Original Paper

Neuropsychobiology 2003;48:136–142
DOI: 10.1159/000073630

Temporomesial Activation in Young Females Associated with Unpleasant Words concerning Body Image

Naoko Shirao[a,c] Yasumasa Okamoto[a,c] Go Okada[a,c] Yuri Okamoto[b]
Shigeto Yamawaki[a,c]

[a]Department of Psychiatry and Neurosciences, Division of Frontier Medical Science, Programs for Biomedical Research, Graduate School of Biomedical Sciences, Hiroshima University, [b]Hiroshima University Health Service Center, Hiroshima, and [c]Core Research for Evolutional Science and Technology (CREST), Japan Science and Technology Corporation (JST), Seika, Japan

Key Words
Amygdala · Parahippocampal gyrus · Functional magnetic resonance imaging · Young women · Body image · Eating disorder

Abstract
Previous behavioral studies suggest that people who have an abnormal eating behavior may perceive information concerning body image distortion more aversively than others. We performed a functional magnetic resonance imaging (fMRI) study on 15 young women, using an emotional decision task including unpleasant words concerning body image and neutral words. The left amygdala and right parahippocampal gyrus were activated by unpleasant words concerning body image relative to neutral words. In addition, activation of the right parahippocampal gyrus was negatively correlated with the severity of psychological and behavioral problems assessed by the Eating Disorder Inventory-2. This activation also positively correlated with the subjects' rating of pleasantness of words concerning body image. These results demonstrated that the temporomesial area plays an important role in the perception of unpleasant words concerning body image. In particular, it is suggested that the right parahippocampal gyrus may be associated with subjective sensitivity to unpleasant information concerning body image.

Introduction

Eating disorder (ED) is characterized not only by aberrant patterns of eating behavior and weight regulation, but also by disturbances in attitudes toward weight and body conformation and in the perception of body shape [1]. A behavioral study showed that restrained eaters who were informed that they were 5 lb (≃2.3 kg) heavier than their actual weight exhibited lower self-esteem, displayed a more negative mood, and ate significantly more food during a subsequent 'taste test' than did other restrained eaters who were informed that they were 5 lb lighter or who were not weighed at all [2]. These results suggest that unpleasant information related to body image strongly influences the pathophysiology of EDs, and that people with an abnormal eating behavior are vulnerable to stressors concerning an unpleasant body and perceive them

KARGER
Fax + 41 61 306 12 34
E-Mail karger@karger.ch
www.karger.com

0302–282X/03/0483–0136$19.50/0

Accessible online at:
www.karger.com/nps

Shigeto Yamawaki, MD, PhD, Department of Psychiatry and Neurosciences
Division of Frontier Medical Science, Programs for Biomedical Research
Graduate School of Biomedical Sciences, Hiroshima University
1-2-3 Kasumi, Minami-ku, Hiroshima, 734-8551 (Japan)
Tel. +81 82 257 5207, Fax +81 82 257 5209, E-Mail yamawaki@hiroshima-u.ac.jp

with more intensity than healthy people. With regard to unpleasant picture stimuli related to body image, a functional magnetic resonance imaging (fMRI) study on female ED patients with a computer-based life image distortion technique revealed that ED patients had greater activity in the right amygdala, right fusiform gyrus and brainstem than healthy female controls when each subject was presented with her own negatively distorted body image [3].

In clinical situations, we often observe that unpleasant words concerning body shape or body weight trigger the onset of an ED, and that these words remain with patients as unpleasant memories. Behavioral studies with tasks requiring word processing using disorder-salient word stimuli have been performed to reveal the specific cognitive pattern of ED patients in processing word stimuli related to body image distortion; these studies found a distorted pattern in the processing of these words in ED patients [4–8].

With regard to neuroimaging studies of emotional linguistic stimuli, a PET study performed during an emotional color Stroop task, in which subjects were instructed to name the color of each word stimulus as either threating or neutral, demonstrated activation of the bilateral amygdalae, left lingual gyrus and posterior parahippocampal gyrus by color-naming of threating words in contrast with neutral words [9]. Furthermore, in an fMRI study using unpleasant and neutral words derived from a database of words [10], Tabert et al. [11] found that the right amygdala and left parahippocampal gyrus showed a blood oxygen level-dependent (BOLD) signal of greater amplitude for unpleasant relative to neutral words during an emotional decision task, in which subjects viewed sets of three unpleasant or three neutral words while selecting the most unpleasant or neutral word, respectively.

However, little is known about the nature of the representations in the human brain for perception of unpleasant words concerning body image, and it is difficult to investigate the possibility of a specific neural substrate underlying the perception of such words even in healthy subjects. Besides, it is not clear whether there is any correlation between the activity of some brain regions and subjects' psychological or behavioral features such as body image distortion, self-esteem, eating behavior and the like.

To determine which areas of the brain are important for the perception of unpleasant words concerning body image and how the severity of psychological and behavioral problems may cause differences in brain activity in the perception of unpleasant word stimuli concerning body image, we used fMRI to investigate brain activation while young female subjects were engaged in an emotional decision task. We hypothesized that the temporomesial area may be involved in the processing of unpleasant words concerning body image used in this study.

Materials and Methods

Subjects

Fifteen women (mean age ± SD, 25.0 ± 3.1 years; range 21–30 years) participated in this study; all were right-handed and native Japanese speakers. Handedness was determined using the Edinburgh Handedness Inventory [12]. Subjects had no history of psychiatric, neurological, or other major medical illness, and had never been treated with psychotropic medication. We limited the study to women from the age of 20 to 30 years, since ED commonly occurs in young females, and since young women are often sensitive to body image information even in the nonclinical population. The average body mass index (BMI) of the 15 subjects was 21.4 (SD 3.6; range 18–31). Their eating behavior, body image distortion and psychological features were assessed by the Japanese version of the Eating Disorder Inventory-2 (EDI-2) [13]. The average score of the total EDI-2 was 41.1 (SD 23.5; range 7–85).

The study was conducted using a protocol that was approved by the Ethics Committee of Hiroshima University School of Medicine. All subjects provided written informed consent for their participation.

Emotional Decision Task

We used the emotional decision task of Tabert et al. [11], with some modification. The words used in this task came from the database of Toglia and Battig [10], which includes 2,854 words that have been rated concerning several items, such as familiarity and pleasantness, from 1 (very unfamiliar; very unpleasant) to 7 (very familiar; very pleasant), with 4 as the midpoint. For the current study, 30 neutral words were selected from the database and translated into Japanese. Thirty highly unpleasant words concerning body image that were selected from Japanese dictionaries and thesauri were also used in this study. These words did not differ significantly in length (mean word length; body vs. neutral = 3.2 vs. 3.1 in Japanese letters) and in familiarity (4.1 vs. 4.3) as shown in our previous research [14]. Both lists contained nouns, verbs, adjectives and adverbs.

The selected words were used to generate both body image and neutral word sets. Each word set comprised a unique combination of 3 words. Word sets were presented in 6 blocks alternating between body image and neutral word sets (3 cycles; fig. 1a). Each block began with a 3-second cue indicating whether the block consisted of unpleasant body image or neutral trials. Five word set trials were presented during each block, each appearing for 4 s with a 1.4-second interstimulus interval (fig. 1b, c). The BOLD response to 3 blocks of body image words and to 3 blocks of neutral words was recorded. During each interstimulus interval, a fixation cross placed centrally replaced the word set. A 9-second resting baseline preceded the first block of trials, during which subjects also viewed a centrally placed fixation cross. During each trial, a word set was projected to the center of the subject's field of view via an SVGA computer-controlled projection system. Presentation timing of word sets was controlled by

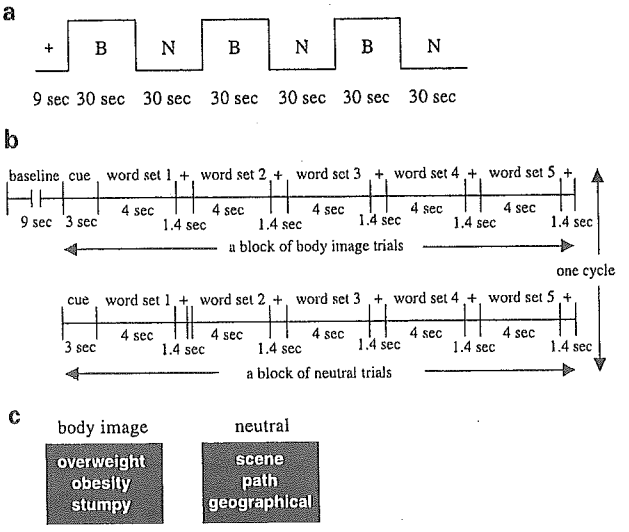

Fig. 1. a Overview of the block-designed stimulus presentation paradigm for the tasks. Six alternating blocks of body image (B) and neutral (N) trials were presented successively. Total scan time was 189 s (3 min and 9 s), while yielding 63 images of 28 axial slices (1,764 images). **b** Blocks of body image and neutral trials preceded by baseline. Each block began with a cue indicating 'body image' or 'neutral'. Subjects were instructed to select a word judged to be the most unpleasant or neutral in each word set, by pressing 1 of 3 buttons. **c** Typical examples of word sets presented in this study. Actual word sets consisted of Japanese words.

Presentation Software Version 0.51 and the word sets were presented in a randomized order.

Immediately before the scanning began, the subjects were given 10 practice trials (5 unpleasant and 5 neutral). Words presented during the practice trial did not overlap with the experimental words.

During body image trials, subjects were instructed to select the most unpleasant word from each word set presented at each trial based on their personal knowledge and experience. During neutral blocks, subjects selected the word they thought to be the most neutral from each word set. Subjects were asked to respond by pressing 1 of 3 buttons on a response pad in the MRI scanner (fig. 1a–c).

Image Acquisition and Postprocessing

fMRI was performed with a Magnex Eclipse 1.5T Power Drive 250 (Shimadzu Medical Systems). A time course series of 63 volumes was acquired with T_2*-weighted, gradient echo, echo planar imaging sequences. Each volume consisted of 28 slices, and the slice thickness was 4.0 mm with no gap, encompassing the whole brain. The interval between two successive acquisitions of the same image (TR) was 3,000 ms, echo time (TE) was 55 ms, and the flip angle was 90°. The field of view was 256 mm, and the matrix size was 64 × 64, giving voxel dimensions of 4.0 × 4.0 × 4.0 mm. After functional scanning, structural scans were acquired using a T_1-weighted gradient echo pulse sequence (TR = 12 ms; TE = 4.5 ms; flip angle = 20°; FOV = 256 mm; voxel dimensions of 1.0 × 1.0 × 1.0 mm), which facilitated localization and coregistration of functional data.

Image processing and statistical analysis were done using the Statistical Parametric Mapping 99 (SPM99) software (Wellcome Department of Cognitive Neurology, London, UK) implemented in Matlab (Mathworks, Inc., Natick, Mass., USA). The first two volumes of the fMRI run (pretask period) were discarded because magnetization was unsteady, and the remaining 61 volumes were used for the statistical analysis. Images were corrected for motion and realigned with the first scan of the session as the reference. T_1 anatomical images were coregistered to first functional images for each subject and aligned to a standard stereotactic space, using the Montreal Neurological Institute (MNI) T_1 template implemented in SPM99. The calculated nonlinear transformation was applied to all functional images for spatial normalization. Finally, the functional images were smoothed with a 12-mm full-width, half-maximum Gaussian filter.

Using group analysis according to a random effect model that allowed inference to general populations [15], we identified regions that showed significant responses during the body image condition vs. the neutral condition as areas related to the cognition of unpleasant word stimuli concerning body image. The resulting set of voxel values for each contrast constituted an SPM(T) map. The SPM(T) maps were then interpreted by referring to the probabilistic behavior of Gaussian random fields. The data were given an initial threshold at an uncorrected $p < 0.001$, and regions about which we had an a priori hypothesis were reported at this threshold [16]. For regions about which there was no clear a priori hypothesis, a more stringent threshold of $p < 0.05$ corrected for multiple comparisons was used. Regions were only reported if they survived at this threshold.

The xyz-coordinates provided by SPM, which are in the MNI brain space, were converted to xyz-coordinates in Talairach and Tournoux's (TT) brain space [17] using the following formula: TT – x = MNI – x × 0.88 – 0.8; TT – y = MNI – y × 0.97 – 3.32; TT – z = MNI – y × 0.05 + MNI – z × 0.88 – 0.44. Labels for brain activation foci were obtained in Talairach coordinates using the Talairach Daemon software, which provides accuracy similar to that of neuroanatomical experts [18]. The labeling of areas given by this software was then confirmed by comparison with activation maps overlaid on MNI-normalized structural MRI images.

Evaluation of Pleasantness and Familiarity of Word Stimuli

Subjects were asked to rate the pleasantness and familiarity of all words presented in these tasks by a 7-point scale immediately after scanning, using a table in which all of the words were printed in randomized order.

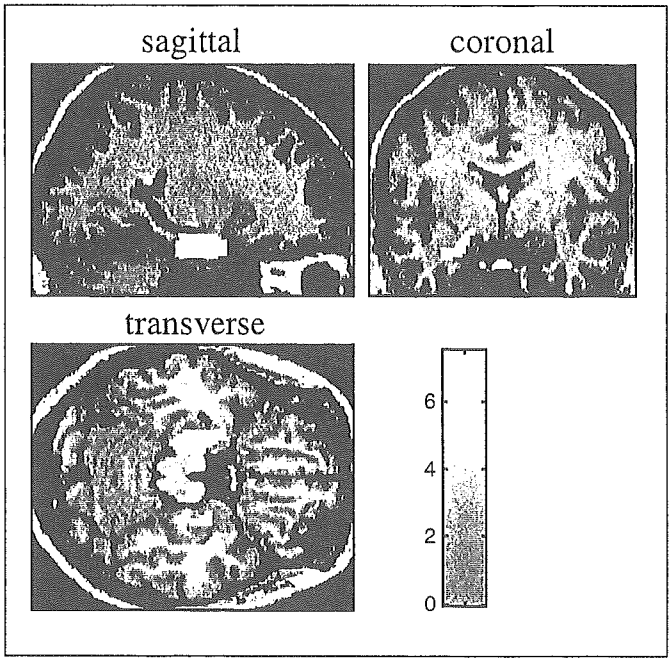

Fig. 2. Statistical parametric maps of brain regions (on the second level group analysis for the 15 subjects) showing significant activation associated with the body image condition compared with the neutral condition at a statistical threshold of an uncorrected $p < 0.001$ (extent of threshold of 80 voxels). Clusters of activation are overlaid onto a T_1-weighted anatomical MR image. T levels of activation are color-coded from red to yellow. The activation in the left amygdala and parahippocampal gyrus and right parahippocampal region are shown.

Table 1. Relative increases in brain activity associated with unpleasant words concerned with body image (task) and neutral words (control)

	Cluster	BA	t score	x	y	z
Lt parahippocampal gyrus	592	28	7.48[a]	−17	−13	−17
(including amygdala)		35	5.11	−18	−29	−21
			4.33	−10	−9	−10
Lt parahippocampal gyrus	562	27	6.66	−6	−32	−4
		30	6.64	−10	−42	−4
Rt parahippocampal gyrus	92	28	5.25	22	−15	−17

x, y, z = Localization according to the standard Talairach coordinates (in mm); BA = Brodmann area; Lt = left; Rt = right.

[a] Area(s) exceeding threshold of $t = 7.31$ ($p < 0.05$ corrected) and all the other areas exceeding the height threshold of $t = 3.79$ ($p < 0.001$ uncorrected) and belonging to a cluster of activation with an extent of at least 80 voxels are displayed.

Results

Rating of Words

Average rating of familiarity did not differ significantly between the two categories of words (mean, body vs. neutral = 4.2 vs. 4.3; $p = 0.19$ by two-tailed Wilcoxon single-rank test). However, subjects rated unpleasant words concerning body image as significantly more unpleasant than neutral words (body vs. neutral = 2.7 vs. 4.2; $p < 0.001$).

Functional MRI Scan

Compared with the neutral condition, the body image condition resulted in the activation of the left parahippocampal gyrus, including the amygdala, and right parahippocampal gyrus (table 1, fig. 2).

Correlation between Brain Activity and Psychological, Behavioral and Biological Data

The BOLD response of the right parahippocampal gyrus to the negative body condition compared with the

Table 2. Correlation between psychological and biological data and the BOLD response of the right parahippocampal gyrus under the body image condition compared with neutral condition

	Correlation coefficient	p value
EDI-2		
Total EDI-2 scores	−0.583	0.022*
Subscales		
Drive for thinness	0.055	0.846
Interoceptive awareness	−0.661	0.007**
Bulimia	−0.563	0.023*
Body dissatisfaction	−0.364	0.183
Ineffectiveness	−0.672	0.006**
Maturity fear	−0.151	0.591
Perfectionism	−0.047	0.868
Interpersonal distrust	−0.611	0.015*
Asceticism	−0.368	0.155
Impulse regulation	−0.533	0.041*
Social insecurity	−0.561	0.030*
Rating of body image words		
Pleasantness	0.551	0.033*
Familiarity	−0.394	0.146
Biological data		
BMI	−0.042	0.881
Age	−0.026	0.928

Correlation coefficients of EDI-2 and rating of body image words were calculated grounded on nonparametric (Spearman) correlation because we used an ordinal scale; coefficients of biological data were based on standard (Pearson) correlation; * $p < 0.05$, ** $p < 0.01$.

neutral condition had a significant negative correlation with total EDI-2 scores (Spearman's rank-order correlation coefficient = −0.583; p = 0.022) and with scores of many subscales of EDI-2, such as interoceptive awareness, bulimia and ineffectiveness (table 2). Furthermore, the BOLD response of this region to the body image condition had a significant positive correlation with the rating of pleasantness of words concerning body image (Spearman's rank-order correlation coefficient = 0.551; p = 0.033). Neither BMI nor age of the subjects correlated with activation of the right parahippocampal gyrus. Besides, no correlation was found between the BOLD response of the left parahippocampal gyrus and EDI-2 scores, nor between BMI and age (table 2).

Discussion

In this study, we used an emotional decision task with unpleasant words concerning body image and neutral words. Previously, we reported that ED patients compared with healthy subjects rated words concerning body image as more unpleasant, although the rating for familiarity did not differ significantly between the two groups. Neither was there a group difference in ratings of pleasantness and familiarity with regard to neutral words [14]. Thus, the task was adequate to examine brain regions that were engaged in the processing of one of the ED-salient stimuli, unpleasant words concerning body image.

The fMRI study revealed that the left parahippocampal gyrus, including the left amygdala, and the right parahippocampal gyrus were associated with the perception of unpleasant words concerning body image.

Compared with the neutral condition, the left amygdala and the surrounding area were activated under the body image condition. Previous studies of patients with a localized brain lesion provided evidence that the human amygdala plays a role in the evaluation of emotional facial expressions related to fear and anger [19, 20], in the evaluation of words denoting negative emotions [21], and in the recognition of nonverbal threat-related sounds [22]. Thus, the young female subjects who participated in this study perceived unpleasant words concerning body image as threat-related, emotionally negative stimuli.

In this study, we detected significant activation in the area of the amygdala only on the left side. Regarding lateralization of emotional processing, previous studies have suggested that the left hemisphere is preferentially involved in positive emotions, whereas the right hemisphere is preferentially involved in negative emotions [23–26]. Recently, however, a hypothesis has been proposed that this right hemisphere dominance may not be fitted to the entire hemisphere but is specific to the prefrontal cortex [27, 28]. Many functional neuroimaging studies using unpleasant linguistic stimuli have shown activation in the left amygdala [29–32] or in the bilateral amygdalae [9], but Tabert et al. [11] reported activation only in the right amygdala. The reason for this discrepancy between the results of Tabert et al. [11] and ours is unclear. However, it may involve differences in word stimuli used in each task and in methods of analysis, including image acquisition and postprocessing. The pattern of the predominant left amygdalar activation caused by unpleasant linguistic materials may be related to left hemisphere dominance for language.

Another possible reason for activation only in the left amygdala in this study is the matter of gender. Several recent neuroimaging studies suggest that gender differences influence the laterality of amygdalar responses in human subjects. For example, a PET study with emotional films [33] and an fMRI study with emotional pictures [34] showed gender differences in the extent to which activity in each amygdala correlates with enhanced memory for emotional stimuli. Both studies suggest that in male subjects, there is a positive correlation between memory enhancement and activation of the right amygdala, while in female subjects, there is a positive correlation between memory enhancement and activation of the left amygdala. Our subjects were all women, and we did not test their memory performance after the fMRI scan. Therefore, recognition of a gender difference was not possible nor could we determine if there was a correlation between brain activity and memory performance. To clarify these points, an additional study is needed that includes male subjects and involves memory performance testing afterwards.

The BOLD response of the right parahippocampal gyrus during the body image condition compared with the neutral condition was correlated positively with the rating of pleasantness of words concerning body image and negatively with the total scores of EDI-2 and with scores of many subscales. A PET study of healthy subjects reporting that the right hemispheric neural network with the temporomesial area including the hippocampus, parahippocampus and amygdala is engaged in ecphory of affect-laden autobiographical information [35] supports our result that the right parahippocampal gyrus was activated in response to the estimation of unpleasant words based on individual past experience. Moreover, the results in our study that the BOLD response in the right parahippocampal gyrus was smaller in subjects with higher EDI-2 scores and in those who rated the words concerning body image as highly unpleasant suggest the possibility that subjects who have a psychological and behavioral dysfunction such as body image distortion and abnormal eating behaviors may have difficulty in tracing their autobiographical information with a negative valence. Interestingly, the correlation analysis on the whole brain showed no correlation between the BOLD response of any brain region and BMI of the subjects. This suggests that the intensity of brain activation while processing the unpleasant information concerning body image may not be determined by actual body shape but by subjective unpleasantness as well as psychological and behavioral problems of the subjects.

Limitations of our study include the relatively low resolution of our data due to the smoothing procedure in order to facilitate intersubject averaging, which made it impossible to attribute the activation to a particular structure. Regarding subjects in this study, in selecting them, we did not use a structured interview. Nevertheless, we made sure that they did not have a psychiatric illness at the time of the study, although we could not rule out such an occurrence in the future. Moreover, because this study included only young female subjects, we could not examine differences between genders or between ED patients and healthy subjects.

Conclusion

Using fMRI, we found that the left amygdala with the surrounding area and the right parahippocampal gyrus were activated in the body image condition in the emotional decision task in 15 healthy young female subjects. In addition, activation of the right parahippocampal gyrus was negatively correlated with the scores of EDI-2 and with the rating of unpleasantness of words concerning body image.

These results suggest the involvement of amygdala in the perception of unpleasant stimuli concerning body image and the possibility of the role of the right parahippocampal gyrus in ecphorizing affect-laden autobiographical information whose activation is negatively correlated with the severity of psychological and behavioral problems.

Further study is needed to compare healthy male with female subjects and to compare healthy subjects with ED patients to reveal any gender differences or elucidate differences in patients with ED.

Acknowledgments

This study was supported by Research on Psychiatric and Neurological Diseases and Mental Health, Ministry of Health Labour and Welfare, Japan.

References

1 American Psychiatric Association: Diagnostic and Statistical Manual of Mental Disorders, ed 4. Washington, American Psychiatric Press, 1994.
2 McFarlane T, Polivy J, Herman CP: Effects of false weight feedback on mood, self-evaluation, and food intake in restrained and unrestrained eaters. J Abnorm Psychol 1998;107:312–318.
3 Seeger G, Braus DF, Ruf M, Goldberger U, Schmidt MH: Body image distortion reveals amygdala activation in patients with anorexia nervosa – A functional magnetic resonance imaging study. Neurosci Lett 2002;326:25–28.
4 Cooper MJ, Anastasiades P, Fairburn CG: Selective processing of eating-, shape-, and weight-related words in persons with bulimia nervosa. J Abnorm Psychol 1992;101:352–355.
5 Cooper MJ, Fairburn CG: Changes in selective information processing with three psychological treatments for bulimia nervosa. Br J Clin Psychol 1994;33:353–356.
6 Cooper M, Todd G: Selective processing of three types of stimuli in eating disorders. Br J Clin Psychol 1997;36:279–281.
7 Jones-Chesters MH, Monsell S, Cooper PJ: The disorder-salient stroop effect as a measure of psychopathology in eating disorders. Int J Eat Disord 1998;24:65–82.
8 Rieger E, Schotte DE, Touyz SW, Beumont PJ, Griffiths R, Russell J: Attentional biases in eating disorders: A visual probe detection procedure. Int J Eat Disord 1998;23:199–205.
9 Isenberg N, Silbersweig D, Engelien A, Emmerich S, Malavade K, Beattie B, Leon AC, Stern E: Linguistic threat activates the human amygdala. Proc Natl Acad Sci USA 1999;96:10456–10459.
10 Toglia MP, Battig WF: Handbook of Semantic Word Norms. Hillsdale, Erlbaum, 1978.
11 Tabert MH, Borod JC, Tang CY, Lange G, Wei TC, Johnson R, Nusbaum AO, Buchsbaum MS: Differential amygdala activation during emotional decision and recognition memory tasks using unpleasant words: An fMRI study. Neuropsychologia 2001;39:556–573.
12 Oldfield RC: The assessment and analysis of handedness: The Edinburgh inventory. Neuropsychologia 1971;9:97–113.
13 Garner DM: Eating Disorder Inventory-2 (EDI-2). Frolida, PAR Inc, 1991.
14 Shirao N, Okamoto Y, Okamoto Y, Otagaki Y, Morinobu S, Yamawaki S: Ratings of negative body image words, negative emotion words and neutral words by eating disorder patients and healthy subjects. Brain Sci Ment Disord 2003;14:141–147.
15 Friston KJ, Holmes AP, Worsley KJ: How many subjects constitute a study? Neuroimage 1999;10:1–5.
16 Elliott R, Friston KJ, Dolan RJ: Dissociable neural responses in human reward systems. J Neurosci 2000;20:6159–6165.
17 Talairach J, Tournoux P: Coplanar Stereotaxic Atlas of the Human Brain. New York, Thieme, 1988.
18 Lancaster JL, Woldorff MG, Parsons LM, Liotti M, Freitas CS, Rainey L, Kochunov PV, Nickerson D, Mikiten SA, Fox PT: Automated Talairach atlas labels for functional brain mapping. Hum Brain Mapp 2000;10:120–131.
19 Adolphs R, Tranel D, Damasio H, Damasio AR: Fear and the human amygdala. J Neurosci 1995;15:5879–5891.
20 Young AW, Aggleton JP, Hellawell DJ, Johnson M, Broks P, Hanley JR: Face processing impairments after amygdalotomy. Brain 1995; 118:15–24.
21 Adolphs R, Russel JA, Tranel D, Damasio AR: A role for the human amygdala in recognizing emotional arousal. Psychol Sci 1999;10:167–171.
22 Scott SK, Young AW, Calder AJ, Hellawell DJ, Aggleton JP, Johnson M: Impaired auditory recognition of fear and anger following bilateral amygdala lesions. Nature 1997;385:254–257.
23 Silberman EK, Weingartner H: Hemispheric lateralization of functions related to emotion. Brain Cogn 1986;5:322–353.
24 Davidson RJ, Ekman P, Saron CD, Senulis JA, Friesen WV: Approach-withdrawal and cerebral asymmetry: Emotional expression and brain physiology. J Pers Soc Psychol 1990;58: 330–341.
25 Borod JC, Bloom RL, Santschi-Haywood C: Verbal aspects of emotional communication; in Beeman M, Chiarello C (eds): Right Hemisphere Language Comprehension: Perspectives from Cognitive Neuroscience. Mahwah, Erlbaum, 1998, pp 285–307.
26 Canli T, Desmond JE, Zhao Z, Glover G, Gabrieli JD: Hemispheric asymmetry for emotional stimuli detected with fMRI. Neuroreport 1998;9:3233–3239.
27 Davidson RJ, Irwin W: The functional neuroanatomy of emotion and affective style. Trends Cogn Sci 1999;3:11–21.
28 Davidson RJ: Anxiety and affective style: Role of prefrontal cortex and amygdala. Biol Psychiatry 2002;51:68–80.
29 Crosson B, Radonovich K, Sadek JR, Gokcay D, Bauer RM, Fischler IS, Cato MA, Maron L, Auerbach EJ, Browd SR, Briggs RW: Left-hemisphere processing of emotional connotation during word generation. Neuroreport 1999;10:2449–2455.
30 Strange BA, Henson RN, Friston KJ, Dolan RJ: Brain mechanisms for detecting perceptual, semantic, and emotional deviance. Neuroimage 2000;12:425–433.
31 Hamann S, Mao H: Positive and negative emotional verbal stimuli elicit activity in the left amygdala. Neuroreport 2002;13:15–19.
32 Moll J, de Oliveira-Souza R, Bramati IE, Grafman J: Functional networks in emotional moral and nonmoral social judgments. Neuroimage 2002;16:696–703.
33 Cahill L, Haier RJ, White NS, Fallon J, Kilpatrick L, Lawrence C, Potkin SG, Alkire MT: Sex-related difference in amygdala activity during emotionally influenced memory storage. Neurobiol Learn Mem 2001;75:1–9.
34 Canli T, Desmond JE, Zhao Z, Gabrieli JD: Sex differences in the neural basis of emotional memories. Proc Natl Acad Sci USA 2002;99: 10789–10794.
35 Fink GR, Markowitsch HJ, Reinkemeier M, Bruckbauer T, Kessler J, Heiss WD: Cerebral representation of one's own past: Neural networks involved in autobiographical memory. J Neurosci 1996;16:4275–4282.

nature neuroscience

Prediction of immediate and future rewards differentially recruits cortico-basal ganglia loops

Saori C Tanaka[1–3], Kenji Doya[1–3], Go Okada[3,4], Kazutaka Ueda[3,4], Yasumasa Okamoto[3,4] & Shigeto Yamawaki[3,4]

Evaluation of both immediate and future outcomes of one's actions is a critical requirement for intelligent behavior. Using functional magnetic resonance imaging (fMRI), we investigated brain mechanisms for reward prediction at different time scales in a Markov decision task. When human subjects learned actions on the basis of immediate rewards, significant activity was seen in the lateral orbitofrontal cortex and the striatum. When subjects learned to act in order to obtain large future rewards while incurring small immediate losses, the dorsolateral prefrontal cortex, inferior parietal cortex, dorsal raphe nucleus and cerebellum were also activated. Computational model–based regression analysis using the predicted future rewards and prediction errors estimated from subjects' performance data revealed graded maps of time scale within the insula and the striatum: ventroanterior regions were involved in predicting immediate rewards and dorsoposterior regions were involved in predicting future rewards. These results suggest differential involvement of the cortico-basal ganglia loops in reward prediction at different time scales.

In daily life, people make decisions based on the prediction of rewards at different time scales; for example, one might do daily exercise to achieve a future fitness goal, or resist the temptation of sweets to avoid future weight gain. Damage to the prefrontal cortex often impairs daily decision making, which requires assessment of future outcomes[1,2]. Lesions in the core of the nucleus accumbens in rats result in a tendency to choose small immediate rewards over larger future rewards[3]. Low activity of the central serotonergic system is associated with impulsive behavior in humans[4], and animals with lesions in the ascending serotonergic pathway tend to choose small immediate rewards over larger future rewards[5,6]. A possible mechanism underlying these observations is that different sub-loops of the topographically organized cortico-basal ganglia network are specialized for reward prediction at different time scales and that they are differentially activated by the ascending serotonergic system[7]. To test whether there are distinct neural pathways for reward prediction at different time scales, we developed a 'Markov decision task' in which an action affects not only the immediate reward but also future states and rewards. Using fMRI, we analyzed brain activity in human subjects as they performed this task. Recent functional brain imaging studies have shown the involvement of specific brain areas, such as the orbitofrontal cortex (OFC) and the ventral striatum, in prediction and perception of rewards[8–11]. In these previous studies, however, rewards were given either independent of the subject's actions or as a function of the current action. Our Markov decision task probes decision making in a dynamic context, with small losses followed by a large positive reward. The results of the block-design analysis suggest differential involvement of brain areas in decision making by prediction of rewards at different time scales. By analyzing subjects' performance data according to a theoretical model of reinforcement learning, we found a gradient of activation within the insula and the striatum for prediction of rewards at different time scales.

RESULTS

Behavioral results

In the Markov decision task, a visual signal (one of three shapes) was presented at the start of each trial to indicate one of three states, and the subject selected one of two actions: pressing the right or left button with the right hand (**Fig. 1a**; see Methods for details). For each state, the subject's action choice affected not only the immediate reward, but also the state subsequently presented (**Fig. 1b,c**).

The rule of state transition was fixed during the entire experiment (**Fig. 1**), but the rules of reward delivery changed according to the task condition. In the SHORT condition, action a_1 gives a small positive reward ($+r_1 = 20$ yen average; see Methods) and action a_2 gives a small loss ($-r_1$) in all three states (**Fig. 1b**). The optimal behavior for maximizing total reward in the SHORT condition is to collect small positive rewards by taking action a_1 at each state. In the LONG condition, action a_2 at state s_3 gives a big bonus ($+r_2 = 100$ yen average; see Methods), and action a_1 at state s_1 results in a big loss ($-r_2$; **Fig. 1c**). The optimal behavior is to receive small losses at state s_1 and s_2 to obtain a large positive reward at state s_3 by taking action a_2 at each state; this is opposite to the optimal behavior in the SHORT condition. Whereas the optimal strategy in the SHORT condition results in small, immediate rewards at each step, the optimal strategy in the LONG condition results in small immediate losses but a net positive reward by the end of one cycle. Thus, for successful action in the LONG condition, subjects must consider both the

[1]Department of Bioinformatics and Genomics, Nara Institute of Science and Technology, 8916-5 Takayama, Ikoma, Nara 630-0101, Japan. [2]Department of Computational Neurobiology, ATR Computational Neuroscience Laboratories, 2-2-2 Hikaridai, Keihanna Science City, Kyoto 619-0288, Japan. [3]CREST, Japan Science and Technology Agency, 2-2-2 Hikaridai, Keihanna Science City, Kyoto 619-0288, Japan. [4]Department of Psychiatry and Neurosciences, Hiroshima University, 1-2-3 Kasumi, Minamiku, Hiroshima 734-8551, Japan. Correspondence should be addressed to K.D. (doya@atr.jp).

Published online 4 July 2004; doi:10.1038/nn1279

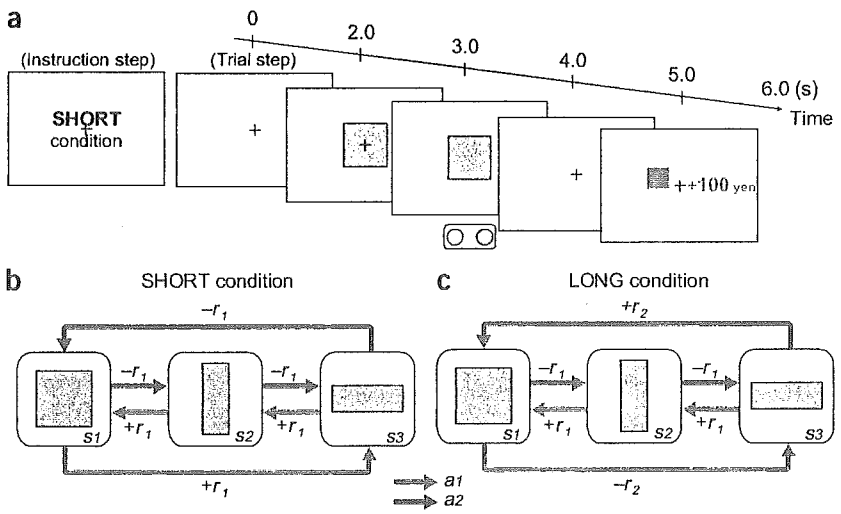

Figure 1 Experimental design. (**a**) Sequences of stimulus and response events in the task. At the beginning of each condition block, the condition is informed by displaying text (6 s), such as 'SHORT condition' (instruction step). In each trial step, a fixation point is presented on the screen, and after 2 s, one of three shapes (square, vertical rectangle or horizontal rectangle) is presented for 1 s. As the fixation point vanishes after 1 s, the subject presses either the right or left button within 1 s. After a short delay (1 s), a reward for that action is presented by a number (indicating yen gained or lost) and the past cumulative reward is shown by a bar graph. Thus, one trial step takes 6 s. (**b**,**c**) The rules of the reward and state transition for action a_1 (magenta arrows) and action a_2 (blue arrows) in the SHORT (**b**) and LONG (**c**) conditions. The small reward r_1 was 10, 20 or 30 yen, with equal probability, and the large reward r_2 was 90, 100, or 110 yen. The rule of state transition was the same for all conditions: $s_3 \rightarrow s_2 \rightarrow s_1 \rightarrow s_3 \ldots$ for action a_1, and $s_1 \rightarrow s_2 \rightarrow s_3 \rightarrow s_1 \rightarrow \ldots$ for action a_2. Although the optimal behaviors are opposite (SHORT: a_1; LONG: a_2), the expected cumulative reward during one cycle of the optimal behavior is 60 yen in both the SHORT ($+20 \times 3$) and LONG (-20, -20, $+100$) conditions.

immediate reward and the future reward expected from the subsequent state, and for success in the SHORT condition, subjects need to consider only the immediate outcome of their actions. Subjects performed 15 trials in a SHORT condition block and 15 trials in a LONG condition block. There were also two control conditions, NO (reward was always zero) and RANDOM (reward was $+r_1$ or $-r_1$, regardless of state or action), so a total of four condition blocks were performed (see **Fig. 2a** for task schedule).

All subjects successfully learned the optimal behaviors: taking action a_1 in the SHORT condition (**Fig. 2b**) and action a_2 in the LONG condition (**Fig. 2c**). Cumulative rewards within each SHORT block (**Fig. 2d**) and LONG block (**Fig. 2e**) also indicate successful learning. It can be seen from the single-subject data in the LONG condition (**Fig. 2e**, orange) that the subject learned to lose small amounts ($-r_1$) twice to get a big bonus ($+r_2$). The average cumulative reward in the last block was 254 yen in the SHORT condition and 257 yen in the LONG condition, which was 84.7% and 85.7%, respectively, of the theoretical optimum of 300 yen.

Block-design analysis

To find the brain areas that are involved in immediate reward prediction, we compared brain activity during the SHORT condition and the NO condition, in which reward was always zero. In the SHORT versus NO contrast, a significant increase in activity was observed in the lateral OFC (**Fig. 3a**), the insula and the occipitotemporal area (OTA) (**Fig. 3b**), as well as in the striatum, the globus pallidus (GP) (**Fig. 3c**) and the medial cerebellum (**Fig. 3d**) (threshold of $P < 0.001$, uncorrected for multiple comparisons). These areas may be involved in reward prediction based on immediate outcome.

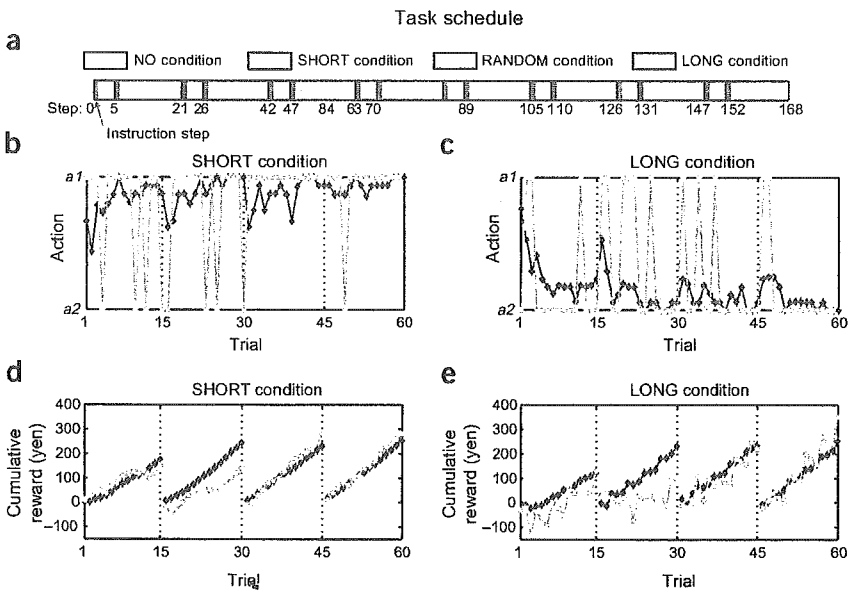

Figure 2 Task schedule and behavioral results. (**a**) A set of four condition blocks—NO (4 trials), SHORT (15 trials), RANDOM (4 trials), LONG (15 trials)—was repeated four times. At the beginning of each condition block, the task condition was presented to the subject (instruction step); thus, the entire experiment consisted of 168 steps (152 trial steps and 16 instruction steps). (**b**,**c**) The selected action of a representative single subject (orange) and the group average ratio of selecting a_1 (blue) in the (**b**) SHORT and (**c**) LONG conditions. (**d**,**e**) The accumulated reward in each block of a representative single subject (orange) and the group average (blue) in the (**d**) SHORT and (**e**) LONG conditions. To clearly show the learning effects, data from four trial blocks in the SHORT and LONG conditions are concatenated, with the dotted lines indicating the end of each condition block.

To identify areas involved in future reward prediction, we compared the brain activity during LONG and SHORT conditions. In the LONG versus SHORT contrast, a robust increase in activity was observed in the ventrolateral prefrontal cortex (VLPFC), the insula, the dorsolateral prefrontal cortex (DLPFC), the dorsal premotor cortex (PMd), the inferior parietal cortex (IPC) (**Fig. 4a**), the striatum, GP (**Fig. 4b**), the dorsal raphe nucleus (**Fig. 4c**), the lateral cerebellum (**Fig. 4d**), the posterior cingulate cortex and the subthalamic nucleus ($P < 0.001$, uncorrected). Activity in the striatum was highly significant (threshold at $P < 0.05$, corrected for a small volume when using an anatomically defined region of interest (ROI) in the striatum; see Methods). These areas are specifically involved in decision making based on the prediction of reward in multiple steps in the future. In the LONG versus NO contrast, the activated areas were approximately the union of the areas activated in the SHORT versus NO and LONG versus SHORT contrasts. These results were consistent with our expectation that both immediate and future reward prediction were required in the LONG condition. The results of block-design analysis, including the LONG versus NO contrast, are summarized in **Supplementary Table 1** online. Activitions in both SHORT and LONG conditions were stronger in the first two blocks, when subjects were involved in active trial and error, than in the last two blocks when the subjects' behavior became repetitive.

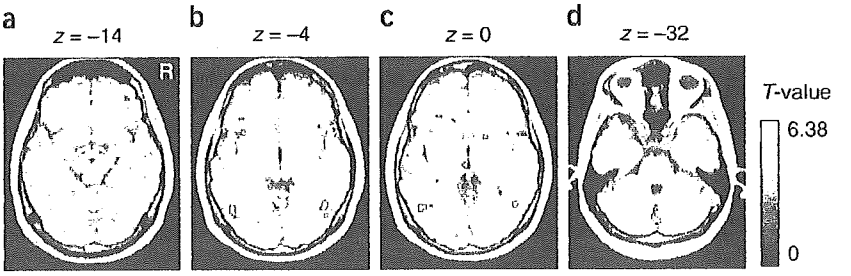

Figure 3 Brain areas activated in the SHORT versus NO contrast ($P < 0.001$, uncorrected; extent threshold of four voxels). (**a**) Lateral OFC. (**b**) Insula. (**c**) Striatum. (**d**) Medial cerebellum.

We compared the activitions in the SHORT versus NO contrast and the LONG versus SHORT contrast, and observed that three regions showed significant activity in both contrasts: the lateral prefrontal cortex (lateral OFC and VLPFC), the insula and the anterior striatum (**Fig. 5**). In the lateral PFC (**Fig. 5a**), although the activities in lateral OFC for the SHORT versus NO contrast (red) and in the VLPFC for the LONG versus SHORT contrast (blue) were close in location, they were clearly separated on the cortical surface. Activities in the insula were also separated (**Fig. 5b**). In the anterior striatum (**Fig. 5c**), we found limited overlaps between the two contrasts (green). In all three areas, activations in the SHORT versus NO contrast were found in the ventral parts, whereas activations in the LONG versus SHORT contrast were found in the dorsal parts.

These results of block-design analysis suggest differential involvement of brain areas in predicting immediate and future rewards.

Performance-based multiple regression analysis

To further clarify the brain structures specific to reward prediction at different time scales, we estimated how much reward the subjects should have predicted on the basis of their performance data and used their time courses as the explanatory variables of regression analysis. We took the theoretical framework of temporal difference (TD) learning[12], which has been successfully used for explaining reward-predictive activations of the midbrain dopaminergic system as well as those of the cortex and the striatum[8,11,13–16]. In TD learning theory, the predicted amount of future reward starting from a state $s(t)$ is formulated as the 'value function'

$$V(t) = E[r(t+1) + \gamma r(t+2) + \gamma^2 r(t+3) + \ldots]. \quad (1)$$

Any deviation from the prediction is given by the TD error

$$\delta(t) = r(t) + \gamma V(t) - V(t-1), \quad (2)$$

which is a crucial learning signal for reward prediction and action selection. The 'discount factor' γ ($0 \leq \gamma < 1$) controls the time scale of prediction: when $\gamma = 0$, only the immediate reward $r(t+1)$ is considered, but as γ approaches 1, rewards in the further future are taken into account.

We estimated the time courses of reward prediction $V(t)$ and prediction error $\delta(t)$ from each subject's performance data and used them as the explanatory variables in multiple regression analysis with fMRI data (see Methods). In our Markov decision task, the minimum value of γ needed to find the optimal action in the LONG condition is 0.36, and any small value of γ is sufficient in the SHORT condition. From the results of our block-design analysis, we assumed that different networks involving the cortex and basal ganglia are specialized for reward prediction at different time scales and that they work in parallel, depending on the requirement of the task. Thus, we varied the discount factor γ as 0, 0.3, 0.6, 0.8, 0.9 and 0.99: small γ for immediate reward prediction and large γ for long future reward prediction. An example of these time courses is shown in **Supplementary Figure 1** online.

We observed a significant correlation with reward prediction $V(t)$ in the medial prefrontal cortex (mPFC; including the anterior cingulate cortex (ACC) and the medial OFC) (**Fig. 6a**) and bilateral insula (**Fig. 6b**), left hippocampus and left temporal pole ($P < 0.001$, uncorrected; see **Supplementary Table 2** online). **Figure 6** shows the correlated

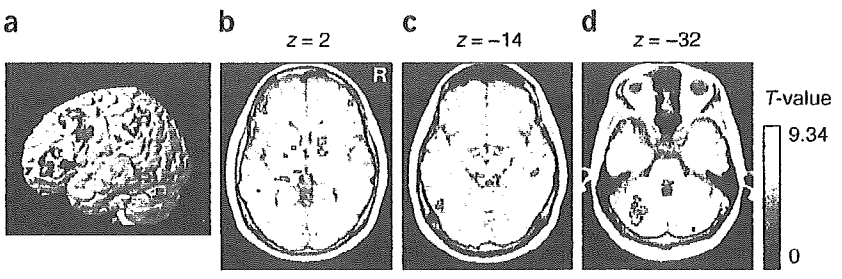

Figure 4 Brain areas activated in the LONG versus SHORT contrast ($P < 0.0001$, uncorrected; extent threshold of four voxels for illustration purposes). (**a**) DLPFC, IPC, PMd. (**b**) GP, striatum. (**c**) Dorsal raphe nucleus. (**d**) Left lateral cerebellum.

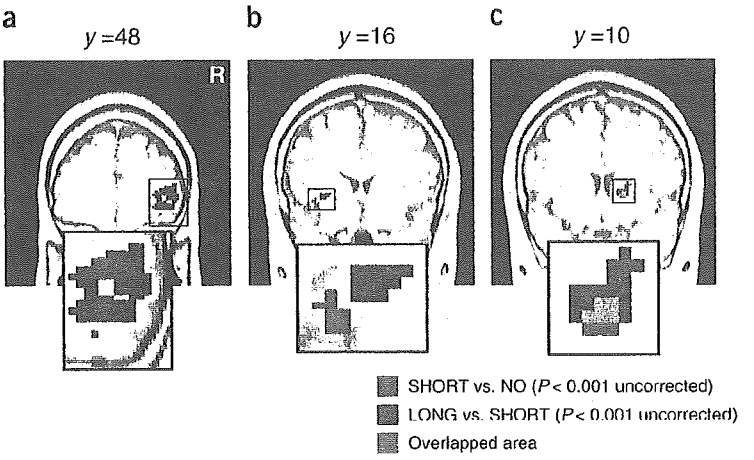

Figure 5 Comparison of brain areas activated in the SHORT versus NO contrast (red) and the LONG versus SHORT contrast (blue). (**a–c**) These figures show activation maps focused on (**a**) the lateral OFC (red (x, y, z) = (38, 46, −14); blue (46, 47, 3)) (**b**) the insula (red (−36, 13, −4); blue (−30, 18, 1)), and (**c**) the striatum (red (18, 10, 0); blue (18, 12, 3)) where we observed significant activation in both contrasts. The areas where activity overlapped area are shown in green.

voxels within these areas using a gradient of colors for different γ values (red for $\gamma = 0$, blue for $\gamma = 0.99$). Activity in the mPFC, temporal pole and hippocampus correlated with reward prediction with a longer time scale ($\gamma \geq 0.6$). Furthermore, in the insula, we found a graded map of activity for reward prediction at different time scales (**Fig. 6b**). Whereas activity in the ventroanterior region correlated with reward prediction at a shorter time scale, activity in the dorsoposterior region correlated with reward prediction at a longer time scale.

We also found, in the basal ganglia, significant correlation with reward prediction error $\delta(t)$ using a wide range of time scales (**Fig. 6c**; $P < 0.001$, uncorrected; see **Supplementary Table 3** online and Methods). Again, we found a graded map, which had a short time scale in the ventroanterior part and a long time scale in the dorsoposterior part. The coincidence of the ventroanterior-dorsoposterior maps and the ventroanterior-dorsoposterior shifts in activities (**Fig. 6b,c**) indicate that, while the ventroanterior regions with smaller γ were predominantly active in the SHORT condition, the dorsoposterior regions with larger γ became more active in the LONG condition.

DISCUSSION

The results of the block-design and performance-based regression analyses suggest differential involvement of brain areas in action learning by prediction of rewards at different time scales. Both block-design and performance-based regression analyses showed activity in the insula and the anterior striatum. Activations of the ventral region in the SHORT versus NO contrast and the dorsal region in the LONG versus SHORT contrast in each area (**Fig. 5**) are consistent with the ventroanterior-dorsoposterior maps of the discount factor γ found in performance-based regression analysis (**Fig. 6**).

The insula takes a pivotal position in reward processing by receiving primary taste and visceral sensory input[17] and sending output to the OFC[18] and the striatum[19]. Previous studies showed that the insula is activated with anticipation of primary reward[10] and that insular lesion causes deficits in incentive learning for primary reward[20]. Our results confirm the role of the insula in prediction of non-primary, monetary reward[21], and further suggest heterogeneous organization within the insula. Previous imaging studies also showed involvement of the insula, especially the ventroanterior region, in processing aversive outcomes[22,23]. Thus a possible interpretation of the activation of the insula in the LONG condition is that it

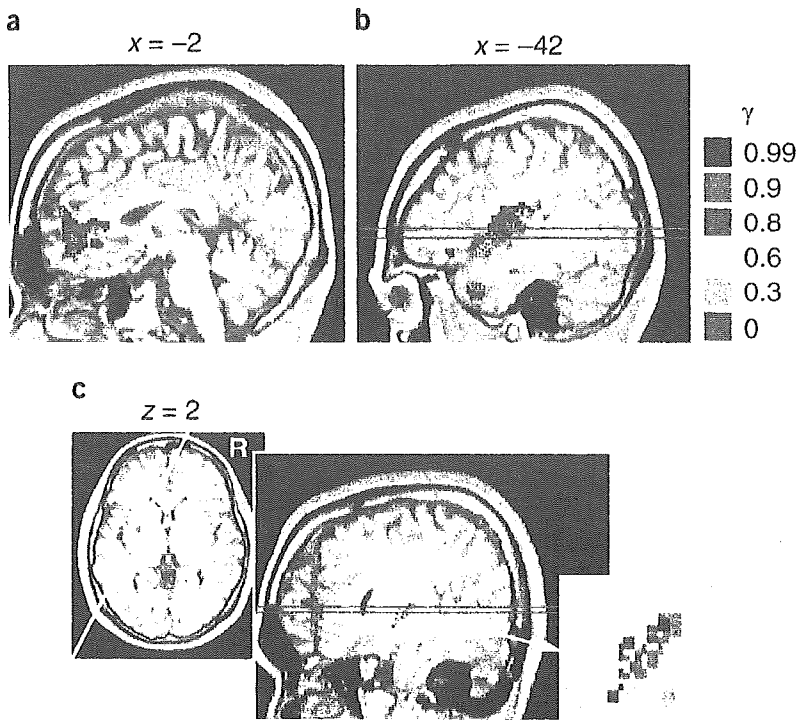

Figure 6 Voxels with a significant correlation (height threshold $P < 0.001$, uncorrected; extent threshold of four voxels) with reward prediction $V(t)$ and prediction error $\delta(t)$ are shown in different colors for different settings of the discount factor γ. Voxels correlated with two or more regressors are shown by a mosaic of colors. (**a**, **b**) Significant correlation with reward prediction $V(t)$. (**a**) mPFC. (**b**) Insula. (**c**) Significant correlation with reward prediction error $\delta(t)$ restricted to ROI in the striatum (slice at white line in horizontal slice at $z = 2$ mm). Note the ventroanterior-to-dorsoposterior gradient with the increase in γ both in the insula and the striatum. Red and blue lines correspond to the z-coordinate levels of activation peaks in the insula and striatum shown in **Figure 5b,c** (red for the SHORT versus NO and blue for the LONG versus SHORT contrasts).